

GAMMA-RADIATION ABSORPTION COEFFICIENTS OF VARIOUS MATERIALS ALLOWING FOR BREMSSTRAHLUNG AND OTHER SECONDARY RADIATIONS

By J. W. ALLISON*

[Manuscript received May 25, 1961]

Summary

Existing calculations of the total absorption coefficient are generally based on the assumption that all the primary radiation energy which is converted into Compton-scattered radiation escapes from the material without significant absorption. This paper extends this basic assumption to include fluorescent and annihilation radiation and bremsstrahlung, and new values of the photoelectric, Compton, pair production, and total absorption coefficients are determined in the energy range 0.01–100 MeV for hydrogen, nitrogen, oxygen, argon, aluminium, iron, lead, air, and water. For comparison purposes revised values of the total absorption coefficient, allowing for the Compton radiation energy loss only, are also determined for these materials, using the most recent data for the component coefficients.

I. INTRODUCTION

When a beam of radiation passes through a material, photoelectric absorption, Compton scattering, and (above 1.02 MeV) pair production take place, as a result of which photons are removed from the beam and energy is absorbed in the material. The fractional loss of photons from an ideally narrow beam of monochromatic radiation per unit path length, and the corresponding fraction of the incident energy which is actually absorbed in the material, are respectively termed the total linear attenuation and total absorption coefficients, μ and μ_a ,† of the material. The values of both these coefficients, or cross sections, depend on the radiation energy as well as on the material. Since some of the energy of the photons removed from the beam is not absorbed but escapes in the form of secondary radiation, $\mu_a < \mu$.

Multiplication of the linear coefficient μ_a by the factors $A/\rho N_0$, $A/\rho N_0 Z$, and $1/\rho$, where A , Z , and ρ are the atomic weight, atomic number, and density in g/cm^3 , and N_0 is Avogadro's number, gives corresponding coefficients per atom, per electron, and per unit mass, ${}_a\mu_a$, ${}_e\mu_a$, and μ_a/ρ respectively. Corresponding expressions hold for the other linear coefficients occurring in this work.

Apart from its importance in measuring the absorption of energy in materials, the absorption coefficient is also of considerable interest in studies of broad-beam attenuation. Under broad-beam conditions the effect of an absorber of thickness x cm is to reduce the dose rate at a given point by the factor $\exp(-\mu_{\text{eff}}x)$, where

* Australian Defence Scientific Service, Defence Standards Laboratories, Department of Supply, Melbourne.

† These coefficients are frequently referred to in the literature as the absorption and the "real" or "true" absorption coefficients, respectively.

μ_{eff} is an effective attenuation coefficient. Since secondary radiation contributes to the dose rate, μ_{eff} must be less than the narrow-beam attenuation coefficient μ , the precise value depending on the absorber geometry. Evans and Evans (1948) have found experimentally that for ^{60}Co gamma-rays, where Compton scattering is the major attenuation process, $\mu_{\text{eff}} = \mu - 0.8\sigma_s = \mu_a + 0.2\sigma_s$, where σ_s is the Compton coefficient relating to the energy carried away by the scattered photons, both when the source is enclosed in a close-fitting cylindrical lead absorber and when a large plane slab of absorber is placed directly against the source. The inequality $\mu_{\text{eff}} > \mu_a$ found in this example is shown in the Appendix to hold in other cases where broad-beam conditions apply and where, in addition to Compton-scattered radiation, the secondary radiation is taken to include fluorescent radiation and bremsstrahlung. Thus in all cases μ and μ_a may be regarded as upper and lower limits to the value of μ_{eff} required to describe the effect of the absorber in reducing the dose-rate. In this sense the coefficients μ and μ_a are of equal interest in problems of broad-beam attenuation.

Grodstein (1957) has made a detailed analysis of theoretical and experimental evidence and has published values of the total mass attenuation coefficient μ/ρ , and the component coefficients τ , σ , and κ , relating to photoelectric absorption, Compton scattering, and pair production respectively. Her work, together with some subsequent revisions by McGinnies (1959), represents the most recent data available and covers a wide range of materials for the energy range 0.01–100 MeV. The results obtained for hydrogen, nitrogen, oxygen, argon, aluminium, iron, lead, air, and water are included in Tables 2 (a), 2 (b), 4, and 5, for comparison with the absorption coefficients calculated for these materials in this paper.

Unlike the attenuation coefficient, which simply represents the probability that a photon will undergo one or other of the three interaction processes, the absorption coefficient cannot be specified uniquely. This is because it is necessary to allow for absorption of the secondary radiations in the material and for escape of the secondary electrons before their energy is dissipated. However, a first approximation may be obtained by assuming that the dimensions of the material are sufficiently great for all the energy of the secondary electrons to be absorbed, but that the secondary radiations escape without significant absorption. The extent to which this basic assumption is realized in practice depends on the dimensions of the material and the energy of the primary radiation.

Existing calculations of the absorption coefficient make use of this assumption to take into account the escape of energy from the material in the form of Compton-scattered radiation. Thus Evans (1955, p. 713) has given graphs of μ_a/ρ for air, water, aluminium, lead, and sodium iodide for the energy range 0.01–100 MeV, which were plotted from the equation

$$\mu_a/\rho = \tau/\rho + \kappa/\rho + \sigma_a/\rho, \quad (1)$$

where $\sigma_a = \sigma - \sigma_s$ is the Compton absorption coefficient relating to the energy which is converted into kinetic energy of secondary electrons in the material.

This calculation takes no account of the fluorescent radiation that is associated with the photoelectric process. In this process a photoelectron is

ejected from the atom and, when the resulting vacancy is filled by an outer shell electron, either an X-ray photon or an Auger electron is emitted by the atom. In heavy materials the emission of radiation predominates: for example, the *K* fluorescent yield, that is, the number of photons which are emitted by the atom per *K* electron vacancy, is about 96% for lead. Also, since electron binding energies are relatively large in such materials, each X-ray photon carries an appreciable amount of energy: about 88 keV for the *K* radiation of lead. Hence an appreciable fraction of the total energy of the primary photons that take part in photoelectric collisions is converted into fluorescent radiation. Moreover, this radiation is sufficiently penetrating for it to travel some distance from its point of origin and should therefore be regarded as escaping from the material like the Compton-scattered radiation. For heavy materials the photoelectric absorption coefficient τ_a is thus substantially less than the attenuation coefficient τ , and at low energies, where the photoelectric process predominates, values of μ_a/ρ calculated from equation (1) are therefore too high.

Following each pair production process two annihilation quanta of total energy $2m_0c^2$, or 1.02 MeV, are produced when the positron, after losing most of its initial kinetic energy, is finally annihilated by an electron. Since this annihilation radiation forms part of the secondary radiation and should also be regarded as escaping from the material, the pair production absorption coefficient κ_a is less than the attenuation coefficient κ . However, although this difference is very large at energies of a few MeV, the error in the total coefficient μ_a/ρ calculated from equation (1) is not more than about 2% since at such energies Compton scattering is the predominant attenuation process. The loss of energy from the material in the form of annihilation radiation is thus relatively unimportant in determinations of the total absorption coefficient.

In discussing the physical significance of the absorption coefficient Evans pointed out that the energy carried away from the primary collisions in the form of degraded secondary photons is not absorbed energy. He also defined energy absorption to mean the photon energy which is converted into kinetic energy of secondary electrons, and stated that this energy is eventually dissipated in the material as heat which could in principle be measured with a calorimeter. At low energies where the energy loss of electrons is predominantly by ionization this view is correct. However, at high energies electrons lose a large part of their energy in the production of bremsstrahlung, that is, secondary radiation emitted when the electron is decelerated or deflected in a nuclear field. Indeed, Heitler (1954, p. 253) has shown that the rate of energy loss per unit path length due to the emission of radiation equals the rate of loss due to ionization at about 10 MeV for lead and at about 125 MeV for water. Thus at high energies, and particularly for heavy materials, an appreciable part of the kinetic energy of the secondary electrons is not dissipated as heat, and it appears that due allowance should be made for this fact.

Some calculations of the total absorption coefficient allowing for all secondary radiations were briefly described by Fano (1953), who published results for water, aluminium, iron, and lead in the energy range 0.088–10 MeV. For heavy materials these results are substantially less than those calculated by taking

Compton-scattered radiation only into account, as would be expected from the above discussion. However, although Evans (1955) dealt with a wider energy range, 0.01–100 MeV, where the effects of fluorescent radiation and bremsstrahlung would be even greater, he did not allow for either of these secondary radiations. Since the results given by Evans have also been included in another textbook by Hine and Brownell (1956), it appears that the importance of fluorescent radiation and bremsstrahlung has not been generally recognized.

The purpose of the present paper is to present new and detailed calculations of the photoelectric, Compton-scattering, pair production, and total absorption coefficients which take into account the loss of energy from the material due to fluorescent radiation, annihilation radiation, and bremsstrahlung, in addition to Compton-scattered radiation. These calculations are based on the underlying assumption referred to earlier. In view of the application of the absorption coefficient in problems concerning the absorption of energy in materials and the fact that this coefficient is also associated with the study of broad-beam attenuation, it is thought that this work should prove of general interest.

II. BREMSSTRAHLUNG CORRECTION FACTORS, $\zeta(T_0)$

In this section, after a brief summary* of existing theoretical results for the probability that an electron of kinetic energy T MeV will produce radiation of energy k MeV, the intensity distribution of the bremsstrahlung is determined for several materials. From this work the rate of radiation energy loss per unit path of the electron $(dT/ds)_{\text{rad}}$ is calculated in units of MeV cm²/g. This is followed by a calculation of the rate of ionization energy loss per unit path of the electron $(dT/ds)_{\text{coll}}$ MeV cm²/g. The values of $(dT/ds)_{\text{rad}}$ and $(dT/ds)_{\text{coll}}$ thus obtained are used to determine the total amount of energy which is spent in ionization when an electron of initial kinetic energy T_0 MeV is brought to rest in each material. Each result is expressed as a bremsstrahlung correction factor $\zeta(T_0)$, which is defined as the ratio of the energy actually absorbed in the material to the initial kinetic energy of the electron. These correction factors, which do not appear to have been determined previously, are employed in the calculations of the photoelectric, Compton-scattering, and pair production absorption coefficients at high radiation energies in the three subsequent sections of this paper. This section concludes with a calculation of the intensity distributions of the total amount of bremsstrahlung emitted when an electron of initial kinetic energy T_0 MeV is brought to rest in each material.

Bethe and Heitler (1934) have shown that in the extreme relativistic region (energies much greater than $\mu_0 = m_0c^2 = 0.51098$ MeV) the cross section $\varphi'(k)dk$ for the emission of a quantum of energy between k and $k+dk$ by an electron of total energy $E = T + \mu_0$ is given by

$$\varphi'(k)dk = \frac{4r_0^2Z^2}{137} \left(1 + \frac{E_f^2}{E^2} - \frac{2E_f}{3E} \right) \left(\ln \frac{2EE_f}{k\mu_0} - \frac{1}{2} \right) \frac{dk}{k}, \quad (2)$$

where $r_0 = e^2/\mu_0 = 2.8178 \times 10^{-13}$ cm and E_f is the final total energy of the electron, provided screening of the nuclear field by the atomic electrons is negligible. At

* A comprehensive review has been given by Koch and Motz (1959).

high energies and with materials of high atomic number the probability of the radiation process taking place at large distances from the nucleus is increased and equation (2) must be modified to take screening into account. For this purpose Bethe and Heitler assumed a Thomas-Fermi distribution of atomic electrons and obtained :

$$2 < \gamma < 15, \quad \varphi'(k)dk = \frac{4r_0^2 Z^2}{137} \left(1 + \frac{E_f^2}{E^2} - \frac{2E_f}{3E} \right) \left[\ln \frac{2EE_f}{k\mu_0} - \frac{1}{2} - c(\gamma) \right] \frac{dk}{k}, \quad (3)$$

$$\gamma < 2, \quad \varphi'(k)dk = \frac{4r_0^2 Z^2}{137} \left\{ \left(1 + \frac{E_f^2}{E^2} \right) \left[\frac{\varphi_1(\gamma)}{4} - \frac{\ln Z}{3} \right] - \frac{2E_f}{3E} \left[\frac{\varphi_2(\gamma)}{4} - \frac{\ln Z}{3} \right] \right\} \frac{dk}{k}, \quad (4)$$

where $\gamma = 100k\mu_0/EE_f Z^{1/3}$ and $\varphi_1(\gamma)$, $\varphi_2(\gamma)$, and $c(\gamma)$ are functions of γ given in Figure 1 and Table 1 of their paper. γ is a measure of the screening: $\gamma \gg 1$ corresponds to the case of no screening; $2 < \gamma < 15$ to that of only slight screening, the function $c(\gamma)$ in equation (3) being a small correction to equation (2); and $\gamma < 2$ to the case where screening is quite appreciable. In the limit of complete screening $\gamma = 0$ and the expression within braces of equation (4) reduces to

$$\left\{ (1 + E_f^2/E^2 - 2E_f/3E) \ln (183Z^{-1/3}) + E_f/9E \right\}.$$

Heitler (1954, p. 254) has considered the various approximations made in the derivation of the preceding equations and has concluded that the only serious error arises from the use of the Born approximation. This approximation has been corrected for in the present work by adding to the expressions the correction δ derived by Davies and Bethe (1952), namely,

$$\delta = - \frac{4 \cdot 828 r_0^2 Z^2}{137} \left(1 + \frac{E_f^2}{E^2} - \frac{2E_f}{3E} \right) f(Z) \frac{dk}{k}, \quad (5)$$

where $f(Z) = (Z/137)^2$ for light materials and $f(Z) = 0.67$ for lead.

In addition to radiation in the field of the nucleus, radiation in the field of the atomic electrons should also be considered. Borsellino (1947) has shown that for the lower energies in the extreme relativistic region where screening is negligible, equation (2) also holds for electrons provided Z^2 is replaced by Z . Thus in this energy region the total cross section is proportional to $Z(Z+1)$. Wheeler and Lamb (1939, 1956) have treated the case of higher energies where screening is appreciable. Assuming a Thomas-Fermi distribution of atomic electrons they found that the cross section $\varphi''(k)dk$ for the emission of a quantum of energy between k and $k+dk$ is given by

$$\varepsilon < 2, \quad \varphi''(k)dk = \frac{4r_0^2 Z}{137} \left\{ \left(1 + \frac{E_f^2}{E^2} \right) \left[\frac{\psi_1(\varepsilon)}{4} - \frac{2 \ln Z}{3} \right] - \frac{2E_f}{3E} \left[\frac{\psi_2(\varepsilon)}{4} - \frac{2 \ln Z}{3} \right] \right\} \frac{dk}{k}, \quad (6)$$

where $\varepsilon = 100k\mu_0/EE_f Z^{2/3}$ and $\psi_1(\varepsilon)$ and $\psi_2(\varepsilon)$ are functions of ε given in Figure 1 of their 1956 paper. In the limit of complete screening $\varepsilon = 0$ and the expression within braces of equation (6) reduces to

$$\left\{ (1 + E_f^2/E^2 - 2E_f/3E) \ln (1440Z^{-2/3}) + E_f/9E \right\}.$$

As a check on the accuracy of the Fermi-Thomas model Wheeler and Lamb used atomic wave functions to recalculate their screening functions ψ_1 and ψ_2 and the corresponding Bethe and Heitler functions φ_1 and φ_2 for nitrogen in the limiting case of high energies (complete screening) and for hydrogen at all energies. This check illustrated the inadequacy of the Fermi-Thomas model for light materials. In the present work the Wheeler and Lamb recalculated values of ψ_1 , ψ_2 , φ_1 , and φ_2 were employed when dealing with hydrogen.

Joseph and Rohrlich (1958) have recently considered the emission of bremsstrahlung, and the analogous process of pair production, where these processes take place in the field of the atomic electrons. Their work indicated that the Wheeler and Lamb calculations are subject to an appreciable error at low energies owing to the neglect of the exchange effect which arises from the similarity of the incident and recoil particles. On the other hand, McGinnies (1959, p. 3) has pointed out that current experimental evidence for pair production supports the Wheeler and Lamb calculations. For this reason the exchange correction derived by Joseph and Rohrlich was not applied in the present work.*

The total intensity $k\varphi(k)$ was calculated in the present investigation for electrons with kinetic energies of 100, 80, 40, 20, 10, and 5 MeV for hydrogen, nitrogen, oxygen, argon, aluminium, iron, and lead. The results for hydrogen, aluminium, and lead, shown graphically in Figure 1, illustrate the intensity distribution of the bremsstrahlung. For convenience the intensity is plotted as a function of k/T , which varies from 0 to 1, rather than of k itself. The curves for lead agree with those given by Heitler (1954, p. 250, Fig. 12) if allowance is made for the fact that his curves do not include the Born correction.

The areas under the intensity distribution curves are a measure of the radiation energy loss $(dT/ds)_{\text{rad}}$ since, in units of MeV cm²/g, this is given by

$$\left(\frac{dT}{ds}\right)_{\text{rad}} = -\frac{N_0}{A} \int_0^1 T k \varphi(k) d\left(\frac{k}{T}\right). \quad (7)$$

Using numerical integration this equation was evaluated for each of the seven materials at the five energies given above. In addition a value of $(dT/ds)_{\text{rad}}$ for an electron with a kinetic energy of 0.1 MeV was obtained from the equation (see Heitler, pp. 251-2, equations (28) and (32))

$$\left(\frac{dT}{ds}\right)_{\text{rad}} = -\frac{16r_0^2 Z^2 N_0 T}{411A}, \quad (8)$$

which holds in the non-relativistic region (energies much less than μ_0). The values of $(dT/ds)_{\text{rad}}$ so obtained for each material were plotted in units of $A/N_0 T$

* Even if the exchange correction were appropriate its omission would not affect the results for the bremsstrahlung correction factors to any significant degree. For heavy materials, radiation in the field of the electrons is small compared with that in the field of the nucleus so that no significant error would occur in the total intensity $\varphi(k) = \varphi'(k) + \varphi''(k)$. In the case of light materials bremsstrahlung in the field of the electrons is more important: indeed for hydrogen it is nearly equal to that in the field of the nucleus. However, the radiation energy loss for this material is small compared with the ionization energy loss so that again no significant error would result in the bremsstrahlung correction factors.

as functions of the energy T and fitted by smooth curves. The results given in Tables 1 (a) and 1 (b) for $(dT/ds)_{\text{rad}}$ in the energy range 0.1–100 MeV were read from these curves, except the results for water which were derived from those for hydrogen and oxygen.

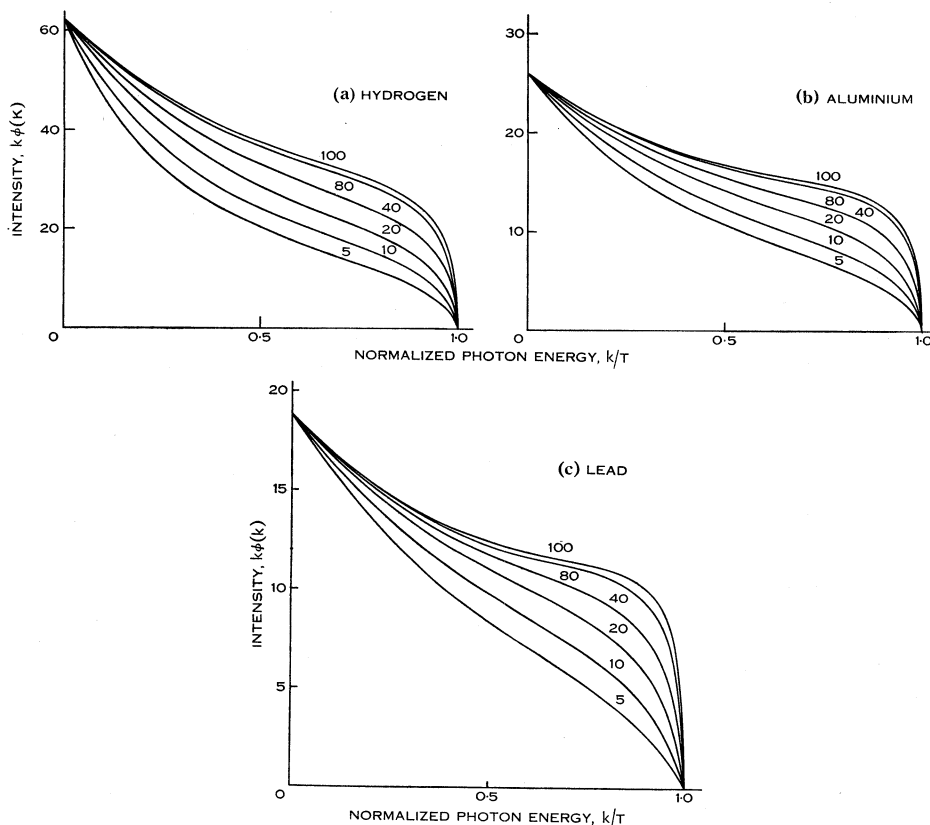


Fig. 1.—Intensity distribution of bremsstrahlung produced by a fast electron. (The ordinates are in units of $r_0^2 Z^2/137$, k is the photon energy, and the numbers affixed to the curves refer to the electron's kinetic energy T MeV.)

The average energy loss per unit path length $(dT/ds)_{\text{coll}}$ of an electron due to excitation and ionization of the atoms of the material through which it travels is given, in units of MeV cm²/g, by the Bethe equation (see Bethe and Ashkin 1953)

$$\left(\frac{dT}{ds}\right)_{\text{coll}} = \frac{2\pi e^4 N_0 Z}{Am_0 v^2} \left\{ \ln \left[\frac{m_0 v^2 T}{2I^2 \lambda^2} \right] - (2\lambda - \lambda^2) \ln 2 + \lambda^2 + \frac{1}{8}(1 - \lambda)^2 \right\}, \quad (9)$$

where v is the velocity of the electron, $\lambda^2 = 1 - (v/c)^2$, and I is the mean excitation potential of the atom. In the present work the ionization loss was calculated for the materials in Tables 1 (a) and 1 (b) using the values of I which Bethe and Ashkin derived from the experimental work of Bakker and Segrè (1951). Values for water were derived from those for hydrogen and oxygen.

TABLE 1 (a)
 RADIATION AND COLLISION ENERGY LOSSES OF AN ELECTRON PER UNIT PATH, $(dT/ds)_{\text{rad}}$ AND
 $(dT/ds)_{\text{coll}}$, FOR GASES*
 Units are MeV cm²/g

Kinetic Energy (MeV)	Hydrogen			Nitrogen		
	Radiation Loss	Collision Loss	Polarization Correction	Radiation Loss	Collision Loss	Polarization Correction
0.1	0.000	8.946		0.001	3.625	
0.2	0.000	5.984		0.001	2.466	
0.5	0.001	4.279		0.003	1.800	
1.0	0.002	3.886		0.008	1.659	
2.0	0.009	3.890		0.022	1.683	
5.0	0.041	4.168		0.078	1.832	
10.0	0.095	4.452		0.177	1.977	
20.0	0.215	4.761		0.390	2.133	
30.0	0.344	4.944	-0.001	0.618	2.226	
40.0	0.477	5.045	-0.029	0.853	2.284	-0.007
50.0	0.617	5.113	-0.065	1.095	2.327	-0.016
60.0	0.756	5.157	-0.103	1.336	2.359	-0.026
80.0	1.042	5.221	-0.170	1.835	2.403	-0.045
100.0	1.334	5.262	-0.231	2.330	2.433	-0.069
Kinetic Energy (MeV)	Oxygen			Argon		
	Radiation Loss	Collision Loss	Polarization Correction	Radiation Loss	Collision Loss	Polarization Correction
0.1	0.001	3.570		0.002	2.908	
0.2	0.001	2.404		0.003	2.000	
0.5	0.004	1.778		0.008	1.477	
1.0	0.009	1.640		0.017	1.373	
2.0	0.025	1.666		0.048	1.404	
5.0	0.087	1.816		0.160	1.543	
10.0	0.196	1.961		0.361	1.674	
20.0	0.435	2.117		0.792	1.815	
30.0	0.691	2.206		1.250	1.900	
40.0	0.954	2.275		1.721	1.958	
50.0	1.225	2.325	-0.002	2.202	2.003	
60.0	1.496	2.359	-0.010	2.683	2.037	-0.005
80.0	2.052	2.412	-0.023	3.664	2.086	-0.015
100.0	2.600	2.445	-0.041	4.661	2.122	-0.026

* Values of the collision loss given in this table include the polarization correction.

TABLE 1 (b)

RADIATION AND COLLISION ENERGY LOSSES OF AN ELECTRON PER UNIT PATH, $(dT/ds)_{\text{rad}}$ AND $(dT/ds)_{\text{coll}}$, FOR CONDENSED MATERIALS*Units are MeV cm²/g

Kinetic Energy (MeV)	Water			Aluminium		
	Radiation Loss	Collision Loss	Polarization Correction	Radiation Loss	Collision Loss	Polarization Correction
0.1	0.001	4.172		0.001	3.231	
0.2	0.001	2.805		0.002	2.214	
0.5	0.004	2.054	-0.004	0.006	1.629	
1.0	0.008	1.865	-0.026	0.014	1.491	-0.003
2.0	0.023	1.849	-0.066	0.038	1.506	-0.034
5.0	0.082	1.925	-0.154	0.128	1.585	-0.102
10.0	0.184	1.996	-0.244	0.287	1.654	-0.173
20.0	0.411	2.063	-0.350	0.636	1.719	-0.258
30.0	0.653	2.096	-0.416	1.005	1.755	-0.312
40.0	0.901	2.124	-0.464	1.382	1.779	-0.351
50.0	1.157	2.144	-0.502	1.772	1.798	-0.382
60.0	1.413	2.160	-0.533	2.161	1.812	-0.408
80.0	1.939	2.184	-0.581	2.946	1.834	-0.449
100.0	2.458	2.203	-0.619	3.741	1.851	-0.482
	Iron			Lead		
	Radiation Loss	Collision Loss	Polarization Correction	Radiation Loss	Collision Loss	Polarization Correction
0.1	0.002	2.896		0.01	2.027	
0.2	0.005	1.969		0.01	1.429	
0.5	0.011	1.471	-0.011	0.03	1.085	
1.0	0.027	1.352	-0.030	0.07	1.024	-0.003
2.0	0.074	1.357	-0.060	0.17	1.056	-0.012
5.0	0.231	1.427	-0.123	0.50	1.152	-0.043
10.0	0.511	1.509	-0.188	1.13	1.230	-0.081
20.0	1.144	1.579	-0.264	2.50	1.305	-0.130
30.0	1.781	1.615	-0.314	3.92	1.345	-0.164
40.0	2.447	1.640	-0.350	5.38	1.371	-0.190
50.0	3.132	1.656	-0.382	6.87	1.390	-0.212
60.0	3.813	1.669	-0.408	8.35	1.405	-0.230
80.0	5.197	1.691	-0.447	11.35	1.428	-0.259
100.0	6.587	1.707	-0.479	14.45	1.445	-0.283

* Values of the collision loss given in this table include the polarization correction.

At high energies the ionization energy loss is appreciably reduced by the shielding effect of the polarization of the medium. This effect has been treated in detail by Sternheimer (1952), who derived a theoretical equation for the correction $(dT/ds)_{\text{pol}}$ which must be added to the values of $(dT/ds)_{\text{coll}}$ obtained from equation (9). The correction is given by

$$\left(\frac{dT}{ds}\right)_{\text{pol}} = -\frac{2\pi e^4 N_0 Z}{A m_0 v^2} \sum_i \left[f_i \ln \left(\frac{\bar{v}_i^2 + l^2}{v_i^2} \right) - l^2 \lambda^2 \right], \quad (10)$$

where f_i is the number of electrons in the i th shell divided by Z , and l is a solution of the equation

$$\frac{\lambda^2}{1-\lambda^2} = \sum_i \frac{f_i}{v_i^2 + l^2}. \quad (11)$$

The frequency \bar{v}_i in equations (10) and (11) is given by Sternheimer as

$$\bar{v}_i = (\pi m_0 A / e^2 N_0 Z)^{1/2} B v_i, \quad (12)$$

where $h\nu_i$ is the excitation potential of the i th shell and B is an empirical correction factor equal to the ratio of the mean excitation potential $I = h\nu_m$ of the atom determined experimentally by Bakker and Segrè to the value deduced from the equation

$$\ln \nu_m = \sum_i f_i \ln \nu_i. \quad (13)$$

Sternheimer calculated the polarization correction for a number of materials and fitted his results by an empirical equation. This empirical equation was used in the present work for the materials in Tables 1 (a) and 1 (b), other than oxygen, for which the values of the coefficients in the empirical equation were not available and the polarization correction was calculated directly from equation (10).

The results obtained in the present work for the ionization loss corrected for polarization are given in Tables 1 (a) and 1 (b), together with results for the polarization correction itself. The values for water and lead agree with those given in graphical form by Heitler (1954, p. 373, Fig. 26). With hydrogen the radiation loss is about 25% of the collision loss for 100 MeV electrons. For heavier materials the radiation loss is even more important. Thus, for 100 MeV electrons, the ratio of the radiation loss to the ionization loss is nearly unity for nitrogen, is about 3.8 for iron, and is as high as 10 for lead.

The energy which is actually absorbed in each material from electrons of energies up to 100 MeV can be derived from the data assembled in Tables 1 (a) and 1 (b). Since the average energy absorbed in a path length ds is given by

$$(dT)_{\text{coll}} = (dT/ds)_{\text{coll}} ds = (dT/ds)_{\text{coll}} (ds/dT)_{\text{total}} (dT)_{\text{total}}, \quad (14)$$

it follows that the average fraction $\zeta(T_0)$ of the initial kinetic energy T_0 MeV which is absorbed when the electron is brought to rest is given by

$$\zeta(T_0) = \frac{1}{T_0} \int_0^{T_0} \left(\frac{dT}{ds}\right)_{\text{coll}} \left(\frac{ds}{dT}\right)_{\text{total}} dT. \quad (15)$$

This integral was evaluated numerically in the present work for the various materials dealt with in this section and the results are given graphically in Figure 2.

This figure shows that for 10 MeV electrons the percentage of energy absorbed in the material due to ionization processes is 99% for hydrogen, 96% for nitrogen, 87% for iron, and 71% for lead. For 100 MeV electrons these percentages become 90, 70, 42, and 23% respectively. It is clear that at high energies, and especially for heavy materials, a substantial part of the initial kinetic energy of the secondary electrons produced in the various radiation attenuation processes is transformed into secondary radiation as the electrons are brought to rest.

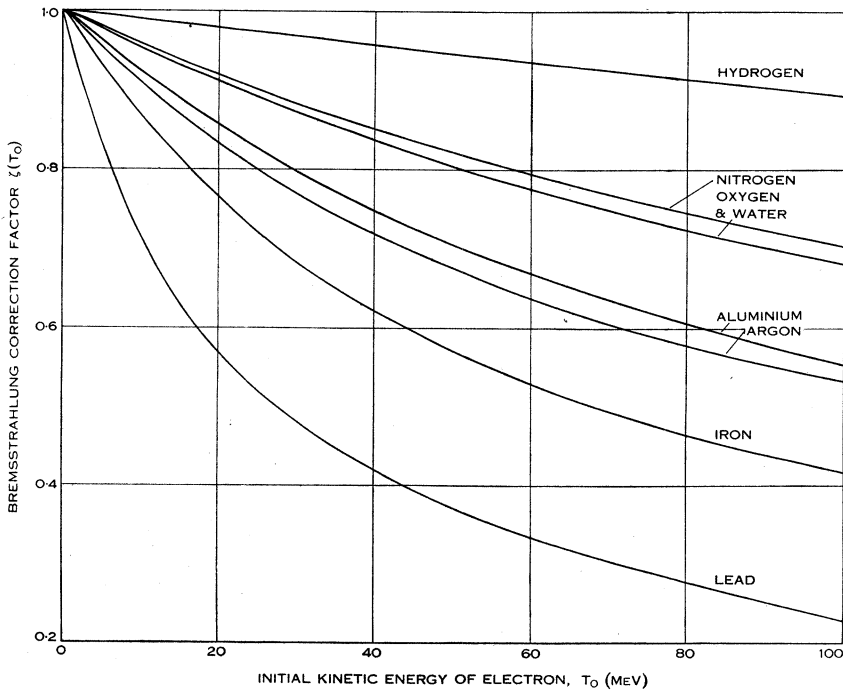


Fig. 2.—Bremsstrahlung correction factors $\zeta(T_0)$ for determining the energy absorbed in a material in which an electron of initial kinetic energy T_0 MeV is brought to rest.

The energy distribution of this radiation may now be derived. As a preliminary step it is necessary to obtain the electron's kinetic energy as a function of the distance travelled by it through the material. When both collision and radiation energy losses are taken into account the distance s , in units of g/cm^2 , which the electron has travelled when its energy has fallen to T MeV, is given by the equation

$$s = \int_T^{T_0} \left\{ 1 / \left(\frac{dT}{ds} \right)_{total} \right\} dT. \tag{16}$$

Using values of $(dT/ds)_{total} = (dT/ds)_{coll} + (dT/ds)_{rad}$ from Tables 1 (a) and 1 (b) this integral can be evaluated numerically for various values of T and T_0 and the required relation between T and s obtained. Thus at each point in its range the kinetic energy of the electron can be found and, from the curves in Figure 1, the corresponding intensity $k\phi(k)$ for the emission of photons of energy k . The

total intensity $k\Phi(k)$ for the emission of photons of energy k as the electron is brought to rest is then given by the equation

$$k\Phi(k) = \frac{N_0}{A} \int_0^{R_0} k\phi(k) ds, \quad (17)$$

where R_0 g/cm², the maximum range of the electron, is given by

$$R_0 = \int_0^{T_0} \left\{ 1 / \left(\frac{dT}{ds} \right)_{\text{total}} \right\} dT. \quad (18)$$

In the present work $k\Phi(k)$ was calculated for initial electron energies of 10, 20, 40, 60, and 100 MeV. The results for aluminium and lead, shown graphically in Figure 3, illustrate the bremsstrahlung intensity distribution. It may be

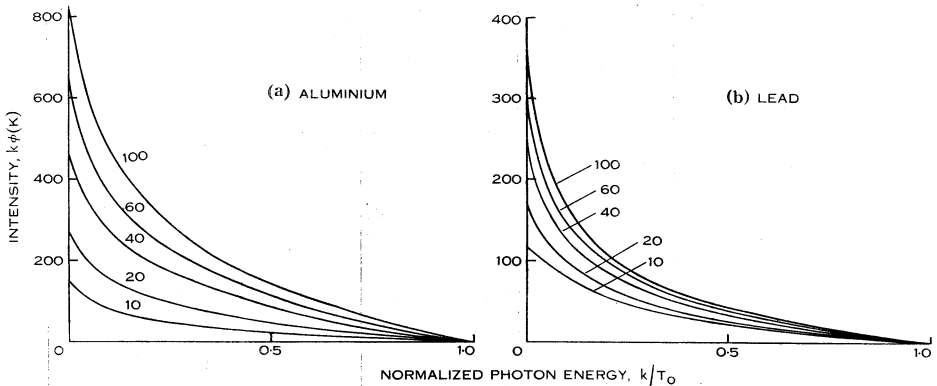


Fig. 3.—Intensity distribution of bremsstrahlung produced by an electron as it is brought to rest. (The ordinates are in units of $r_0^2 Z^2 N_0 / 137A$, k is the photon energy, and the numbers affixed to the curves refer to the electron's initial kinetic energy T_0 MeV.)

noted that the areas under these curves are a measure of the total amount of energy E_R MeV converted into radiation, since this is given by

$$E_R = \int_0^1 T_0 k \Phi(k) d\left(\frac{k}{T_0}\right). \quad (19)$$

The bremsstrahlung correction factors $\zeta(T_0)$, which are simply equal to $(T_0 - E_R)/T_0$, may therefore be obtained from the results illustrated in Figure 3. However, the preceding calculation of these factors is more direct and more accurate.

III. PHOTOELECTRIC ABSORPTION COEFFICIENT

Values of the photoelectric absorption coefficient τ_a are derived in this section of the paper from those for the attenuation coefficient τ given by Grodstein and McGinnies (see Tables 2 (a) and 2 (b)) by applying a correction for the escape of energy in the form of fluorescent radiation from each material. A further correction is made in the case of lead to allow for the energy carried away in the form of bremsstrahlung, since for this material the photoelectric process remains significant up to fairly high energies.

The amount of primary energy which is converted into fluorescent radiation is negligible at all energies for the materials in Table 2 (a), since, firstly, the production of Auger electrons (Burhop 1954) predominates over that of X-ray photons, that is, only a few photoelectric collisions are accompanied by the emission of radiation, and secondly, electron binding energies are small so that each X-ray photon which is emitted carries only a small amount of energy. For example, for 10 keV primary radiation, and for aluminium which has a *K* fluorescent yield of about 0.031 and a *K* electron binding energy of about 1.56 keV, only about 0.5% of the primary energy is transformed into fluorescent radiation. This proportion is even less for greater primary energies, or for lighter materials which have smaller fluorescent yields and electron binding energies. Moreover, even the small amount of fluorescent radiation which is produced cannot be considered as escaping from the material since, because of its softness, it is absorbed within a very short distance of its point of origin. Thus for all the materials in Table 2 (a) the fluorescent radiation correction is negligible and the photoelectric absorption and attenuation coefficients are equal.

Appreciable corrections are required for the heavier materials in Table 2 (b) which have greater fluorescent yields and electron binding energies. For primary radiation energies greater than the *K* absorption limit of the material the photoelectron can be ejected from any of the shells of the atom so that *K*, *L*, *M*, . . . fluorescent radiations are produced. However, the fluorescent yield, the binding energy of an electron, and the probability for the photoelectric process itself

TABLE 2 (a)
MASS PHOTOELECTRIC ATTENUATION COEFFICIENTS τ/ρ FOR LIGHT MATERIALS*†

Energy (MeV)	τ/ρ (cm ² /g)					
	Hydrogen	Nitrogen	Oxygen	Aluminium	Air	Water
0.01	0.0027	3.31	5.34	25.56	4.55	4.75
0.015	0.0007	0.877	1.44	7.48	1.25	1.28
0.02		0.345	0.561	3.04	0.495	0.498
0.03		0.0912	0.152	0.855	0.135	0.135
0.04		0.0340	0.0557	0.324	0.0505	0.0495
0.05		0.0159	0.0263	0.156	0.0240	0.0234
0.06		0.0086	0.0147	0.0870	0.0133	0.0130
0.08		0.0034	0.0056	0.0350	0.0052	0.0050
0.10		0.0017	0.0026	0.0172	0.0026	0.0024
0.15		0.0004	0.0008	0.0047	0.0007	0.0007
0.20			0.0004	0.0018	0.0002	0.0003
0.30				0.0004		
0.40				0.0002		

* All values are directly from Grodstein (1957) and McGinnies (1959), except the values for air which are derived from those for nitrogen, oxygen, and argon.

† For these materials the photoelectric absorption coefficient τ_a/ρ equals the attenuation coefficient.

TABLE 2 (b)

MASS PHOTOELECTRIC ATTENUATION AND ABSORPTION COEFFICIENTS, τ/ρ AND τ_a/ρ , FOR HEAVY MATERIALS*Units are cm^2/g

Energy (MeV)	Argon		Iron		Lead†	
	τ/ρ	τ_a/ρ	τ/ρ	τ_a/ρ	τ/ρ	τ_a/ρ
0.01	64.0	62.0	179	141	137	137
0.01307					67.6	67.6
0.015	19.6	19.2	57.7	49.4		
0.01589					168	115
0.02	8.19	8.07	25.0	22.2	90.0	68.1
0.03	2.43	2.40	7.74	7.19	30.5	25.7
0.04	0.935	0.929	3.30	3.13	14.3	12.5
0.05	0.460	0.457	1.64	1.57	7.82	7.09
0.06	0.264	0.262	0.960	0.926	4.59	4.24
0.08	0.107	0.107	0.404	0.303	2.00	1.88
0.08823					{ 1.52	1.44
					{ 7.30	1.36
0.10	0.054	0.054	0.204	0.199	5.17	1.49
0.15	0.0148	0.015	0.058	0.057	1.73	0.886
0.20	0.0062	0.0062	0.0240	0.0238	0.799	0.501
0.30	0.0018	0.0018	0.0071	0.0071	0.272	0.204
0.40	0.0008	0.0008	0.0031	0.0031	0.133	0.107
0.50	0.0005	0.0005	0.0017	0.0017	0.0759	0.0641
0.60	0.0003	0.0003	0.0011	0.0011	0.0503	0.0435
0.80			0.0005	0.0005	0.0276	0.0244
1.0			0.0003	0.0003	0.0180	0.0161
1.5					0.0087	0.0080
2.0					0.0058	0.0051
3.0					0.0032	0.0029
4.0					0.0023	0.0020
5.0					0.0017	0.0014
6.0					0.0014	0.0011
8.0					0.0010	0.0010
10					0.0008	0.0006
15					0.0005	0.0003
20					0.0004	0.0002
30					0.0003	0.0002
40					0.0002	0.0001
50					0.0001	0.0001

* Values of τ/ρ are from Grodstein (1957) and McGinnies (1959).† For this material the values given for 0.01 and 0.01307 MeV (L_3 edge) are for the M shell; from 0.01589 MeV (L_1 edge) to 0.08823 MeV (K edge) they are for the L and M shells; and from 0.08823 MeV upwards they are for the K , L , and M shells.

are all less for an outer shell than for the *K* shell, so that little energy is converted into radiations other than the *K*. Hence it is only necessary to allow for the escape of *K* radiation. In the case of lead the energy range 0.01–100 MeV extends below both the *K* and *L* absorption limits (0.08823 and 0.01307 MeV). For this material and energies in the range 0.01307–0.08823 MeV the *L* fluorescent radiation must be taken into account since, firstly, the photoelectric process occurs predominantly in the *L* shell and secondly, the energy of the *L* radiation (about 15 keV) is appreciable compared to the primary energy. For energies less than 0.01307 MeV the photoelectric process occurs predominantly in the *M* shell and, since the fluorescent yield of this shell is very small (Burhop quotes the value 0.06 for uranium), the fluorescent radiation correction is negligible.

Hence for primary energies $h\nu$ greater than the *K* absorption limit of the material, and for energies between the *K* and *L* absorption limits in the case of lead, the photoelectric absorption coefficient is given by the respective equations

$$\frac{\tau_a}{\rho} = \frac{h\nu - p_K \omega_K I_K}{h\nu} \frac{\tau}{\rho}, \tag{20}$$

and

$$\frac{\tau_a}{\rho} = \frac{h\nu - p_L \omega_L I_L}{h\nu} \frac{\tau}{\rho}, \tag{21}$$

where $p_K = \tau_K / \tau_{K+L+M}$ and $p_L = \tau_L / \tau_{L+M}$ are the fractions of the total number of photoelectric collisions which occur in the *K* and *L* shells, ω_K and ω_L are the *K* and *L* fluorescent yields, and I_K and I_L are the ionization potentials of the *K* and *L* shells.

For the present calculation, values of I_K and I_L , ω_K , and p_K were obtained from the works of Hill, Church, and Mihelich (1952), Broyles, Thomas, and Haynes (1953), and Grodstein (1957, p. 18, Table V) respectively. The value of ω_L required in equation (21) was obtained from the early work of Lay (1934), who used X-ray excitation to find the fluorescent yields of several materials.* No information was available in the literature for the fraction p_L required in equation (21) and this was calculated with the aid of the Hall (1936) equations for the photoelectric attenuation coefficients of the *L* and *M* shells. These equations are respectively

$$\tau_L = \frac{2^{14} A_0}{(Z - s_2)^2} v_2^4 (1 + 6v_2 + 8v_2^2) \frac{\exp \{-8(v_1/v) \arctan (v/v_1)\}}{1 - \exp (-4\pi v_1/v)}, \tag{22}$$

and

$$\tau_M = \frac{2^9 A_0 3^3}{(Z - s_3)^2} v_3^4 (1 + 8v_3)(27 + 136v_3 + 208v_3^2 + 96v_3^3) \frac{\exp \{-4n_3 \arctan (3/n_3)\}}{1 - \exp (-2\pi n_3)}, \tag{23}$$

* Although the determination of *K* fluorescent yields has been the subject of considerable work, little information is available concerning the yields of outer shells. Lay's work has recently been supported by a value of ω_L for lead obtained by Patronis, Braden, and Wyly (1957). On the other hand values of ω_L published by Robinson and Fink (1955) for several materials do not agree with Lay's results, possibly because nuclear rather than X-ray excitation was employed.

where $A_0 = h^3 N_0 \rho / 12 \pi m_0^2 c A e^2$, $v_2 = (Z - s_2)^2 / 4\nu$, $v_1 = \pi e^2 (Z - s_2) / h$, $v/v_1 = (1/v_2 - 1)^{1/2}$, $v_3 = (Z - s_3)^2 / 9\nu$, $n_3 = 3(1/v_3 - 1)^{-1/2}$, and s_2 and s_3 are Slater screening constants. A check on the calculation of τ_L and τ_M was provided by the fact that the sum $\tau_L + \tau_M$ was found to be in good agreement with the values of τ calculated independently by Grodstein.

The results obtained for the photoelectric absorption coefficients of argon, iron, and lead are given in Table 2 (b). In the case of lead these results include a correction for the bremsstrahlung produced in this material by high energy photoelectrons. This correction was made by subtracting an amount

$$\frac{E_R}{h\nu} \frac{\tau}{\rho} = \frac{T_0}{h\nu} [1 - \zeta(T_0)] \frac{\tau}{\rho}, \quad (24)$$

where $T_0 = h\nu - I_K$, from the values of τ_a/ρ obtained from equation (20).

Comparison of the values of τ_a/ρ and τ/ρ given in Table 2 (b) indicates the effect of taking fluorescent radiation and bremsstrahlung into account. The greatest change is for lead; for an energy just greater than the K absorption limit of this material, τ_a/ρ is only 19% of τ/ρ .

IV. COMPTON ABSORPTION COEFFICIENT

Although the variation in the energy and the number of Compton-scattered photons with the angle through which they are scattered have been considered frequently in the literature, the most comprehensive treatment being that of Nelms (1953), no information appears to be available giving the intensity distribution as a function of the radiation energy. This distribution is of interest in the present work, since the validity of the assumption that the scattered radiation escapes from the material without significant absorption depends on the energy of the radiation. This section contains a derivation of the radiation energy distribution, and a new calculation of the Compton absorption coefficient which allows for the loss of energy from the material in the form of bremsstrahlung.

The number of photons $g(\theta)d\Omega$ which are scattered by an electron through an angle θ into a small solid angle $d\Omega$ is given by the well known Klein-Nishina equation

$$g(\theta)d\Omega = \frac{r_0^2}{2} \left\{ \frac{(1 + \cos^2 \theta)[1 + \alpha(1 - \cos \theta)] + \alpha^2(1 - \cos \theta)^2}{[1 + \alpha(1 - \cos \theta)]^3} \right\} d\Omega, \quad (25)$$

where $\alpha = h\nu/\mu_0$ and $h\nu$ is the primary radiation energy. The energy $h\nu'$ of the scattered photon is given by the Compton equation

$$h\nu' = h\nu/[1 + \alpha(1 - \cos \theta)]. \quad (26)$$

From equations (25) and (26) it can be shown that the number of photons $g(h\nu')d(h\nu')$ which are scattered per electron so that they have an energy between $h\nu'$ and $h\nu' + d(h\nu')$ is given by the equation

$$g(h\nu')d(h\nu') = \frac{\pi r_0^2}{\alpha h\nu} \left[\frac{1}{\alpha^2} \left(\frac{h\nu}{h\nu'} \right)^2 + \left(1 - \frac{2}{\alpha} - \frac{2}{\alpha^2} \right) \frac{h\nu}{h\nu'} + \left(\frac{2}{\alpha} + \frac{1}{\alpha^2} \right) + \frac{h\nu'}{h\nu} \right] d(h\nu'). \quad (27)$$

The required cross section $g'(h\nu')d(h\nu')$ for the energy scattered per electron in the range $d(h\nu')$ is given by the equation

$$g'(h\nu')d(h\nu') = (h\nu'/h\nu)g(h\nu')d(h\nu'). \tag{28}$$

The intensity $g'(h\nu')$ was calculated in the present work for primary radiation energies of 0.1, 1, 10, and 100 MeV. The results, given graphically in Figure 4, illustrate the energy distribution of the Compton-scattered radiation. For convenience the intensity is plotted as a function of $h\nu'/h\nu$, which varies from 0 to 1, rather than of $h\nu'$ itself.

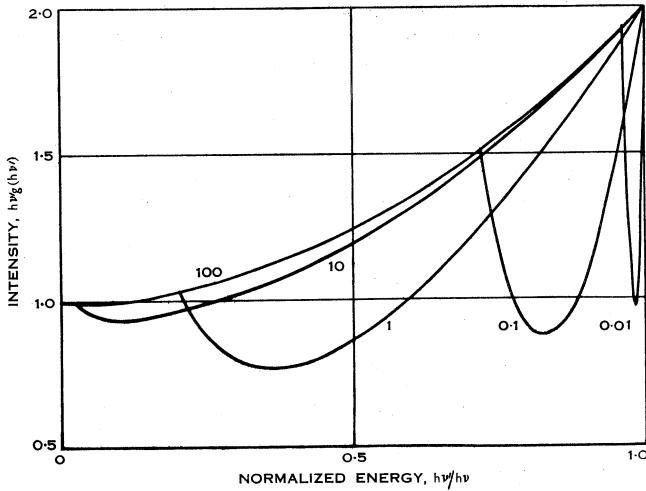


Fig. 4.—Intensity distribution of Compton-scattered photons. (The ordinates are in units of $\pi r_0^2/\alpha$, $h\nu'$ is the energy of the scattered photon, and the numbers affixed to the curves refer to the primary radiation energy $h\nu$ in MeV.)

Reference to Figure 4 shows that at high primary energies the scattered radiation contains a considerable amount of relatively soft photons. Thus, whereas for 0.01 MeV radiation the minimum scattered photon energy is about 96% of the primary energy, for 0.1, 1, 10, and 100 MeV radiation it falls to about 75, 20, 2.5, and 0.25% respectively. Again, consideration of the areas* under the curves in this figure shows that for primary energies of 10 and 100 MeV about 30 and 40% respectively of the total scattered energy are carried by photons with energies less than half the primary energy.

* The total area under each of these curves represents the Compton cross section σ_s for the total amount of energy which is scattered by each electron in the material. However, this cross section is better obtained analytically from the equation

$$\sigma_s = \int_0^1 h\nu'g'(h\nu')d(h\nu'/h\nu).$$

The cross-section $g''(h\nu')d(h\nu')$ for the energy converted into kinetic energy of secondary electrons in the range $d(h\nu')$ is given by the equation

$$g''(h\nu')d(h\nu') = \{(h\nu - h\nu')/h\nu\}g(h\nu')d(h\nu'). \tag{29}$$

Analytical integration gives the well known Klein-Nishina equation for the total cross section ${}_e\sigma_a$, namely,

$${}_e\sigma_a = \pi r_0^2 \left[\frac{-20\alpha^4 + 102\alpha^3 + 186\alpha^2 + 102\alpha + 18}{3\alpha^2(1+2\alpha)^3} + \frac{\alpha^2 - 2\alpha - 3}{\alpha^3} \ln(1+2\alpha) \right]. \tag{30}$$

TABLE 3

COMPTON MASS ABSORPTION COEFFICIENT σ_a/ρ ALLOWING FOR THE ESCAPE FROM THE MATERIAL OF (a) SCATTERED RADIATION ONLY AND (b) SCATTERED RADIATION AND BREMSSTRAHLUNG

Units are cm^2/g

Energy (MeV)	σ_a/ρ													
	Hydrogen		Nitrogen, Oxygen, and Air		Aluminium		Argon		Iron		Lead		Water	
	(a)	(b)	(a)	(b)	(a)	(b)	(a)	(b)	(a)	(b)	(a)	(b)	(a)	(b)
0.01	0.0072	0.0072	0.0036	0.0036	0.0035	0.0035	0.0033	0.0033	0.0034	0.0034	0.0029	0.0029	0.0040	0.0040
0.01307											0.0036	0.0036		
0.015	0.0104	0.0104	0.0052	0.0052	0.0050	0.0050	0.0047	0.0047	0.0049	0.0049	0.0041	0.0041	0.0058	0.0058
0.01589											0.0044	0.0044		
0.02	0.0133	0.0133	0.0068	0.0068	0.0065	0.0065	0.0061	0.0061	0.0062	0.0062	0.0053	0.0053	0.0074	0.0074
0.03	0.0186	0.0186	0.0094	0.0094	0.0090	0.0090	0.0084	0.0084	0.0087	0.0087	0.0074	0.0074	0.0104	0.0104
0.04	0.0231	0.0231	0.0116	0.0116	0.0112	0.0112	0.0105	0.0105	0.0108	0.0108	0.0092	0.0092	0.0129	0.0129
0.05	0.0271	0.0271	0.0136	0.0136	0.0132	0.0132	0.0123	0.0123	0.0127	0.0127	0.0108	0.0108	0.0152	0.0152
0.06	0.0305	0.0305	0.0154	0.0154	0.0148	0.0148	0.0139	0.0139	0.0143	0.0143	0.0122	0.0122	0.0171	0.0171
0.08	0.0362	0.0362	0.0182	0.0182	0.0176	0.0176	0.0164	0.0164	0.0170	0.0170	0.0144	0.0144	0.0203	0.0203
0.08823											0.0151	0.0151		
0.10	0.0406	0.0406	0.0205	0.0205	0.0197	0.0197	0.0185	0.0185	0.0191	0.0191	0.0162	0.0162	0.0227	0.0227
0.15	0.0481	0.0481	0.0242	0.0242	0.0234	0.0234	0.0219	0.0219	0.0226	0.0226	0.0192	0.0192	0.0269	0.0269
0.20	0.0525	0.0525	0.0265	0.0265	0.0255	0.0255	0.0239	0.0239	0.0246	0.0246	0.0210	0.0210	0.0294	0.0294
0.30	0.0569	0.0569	0.0287	0.0287	0.0277	0.0277	0.0259	0.0259	0.0267	0.0267	0.0227	0.0227	0.0319	0.0319
0.40	0.0586	0.0586	0.0295	0.0295	0.0285	0.0285	0.0266	0.0266	0.0275	0.0275	0.0234	0.0234	0.0328	0.0328
0.50	0.0590	0.0590	0.0297	0.0297	0.0286	0.0286	0.0268	0.0268	0.0277	0.0277	0.0235	0.0235	0.0330	0.0330
0.60	0.0587	0.0587	0.0296	0.0296	0.0285	0.0285	0.0267	0.0267	0.0276	0.0276	0.0234	0.0234	0.0329	0.0329
0.80	0.0574	0.0574	0.0289	0.0289	0.0279	0.0279	0.0261	0.0261	0.0269	0.0269	0.0229	0.0227	0.0321	0.0321
1.0	0.0555	0.0555	0.0280	0.0280	0.0270	0.0269	0.0252	0.0252	0.0260	0.0260	0.0222	0.0218	0.0311	0.0311
1.5	0.0507	0.0507	0.0255	0.0255	0.0246	0.0246	0.0230	0.0230	0.0238	0.0237	0.0202	0.0197	0.0284	0.0284
2.0	0.0464	0.0464	0.0234	0.0234	0.0225	0.0224	0.0211	0.0210	0.0218	0.0215	0.0185	0.0176	0.0260	0.0260
3.0	0.0397	0.0397	0.0200	0.0199	0.0193	0.0190	0.0180	0.0177	0.0186	0.0182	0.0158	0.0148	0.0222	0.0222
4.0	0.0348	0.0348	0.0175	0.0174	0.0169	0.0166	0.0158	0.0154	0.0163	0.0157	0.0139	0.0125	0.0195	0.0193
5.0	0.0311	0.0311	0.0157	0.0155	0.0151	0.0147	0.0141	0.0137	0.0146	0.0139	0.0124	0.0109	0.0174	0.0172
6.0	0.0282	0.0282	0.0142	0.0140	0.0137	0.0132	0.0128	0.0123	0.0132	0.0125	0.0112	0.0097	0.0158	0.0156
8.0	0.0239	0.0238	0.0120	0.0118	0.0116	0.0111	0.0108	0.0103	0.0112	0.0103	0.0095	0.0076	0.0134	0.0131
10	0.0208	0.0208	0.0105	0.0103	0.0101	0.0095	0.0095	0.0089	0.0098	0.0088	0.0083	0.0062	0.0117	0.0113
15	0.0160	0.0159	0.0081	0.0075	0.0078	0.0071	0.0072	0.0066	0.0075	0.0064	0.0064	0.0043	0.0089	0.0083
20	0.0131	0.0130	0.0066	0.0062	0.0064	0.0056	0.0060	0.0052	0.0062	0.0050	0.0052	0.0032	0.0073	0.0069
30	0.0098	0.0096	0.0049	0.0044	0.0048	0.0039	0.0045	0.0038	0.0046	0.0033	0.0039	0.0021	0.0055	0.0049
40	0.0079	0.0077	0.0040	0.0034	0.0039	0.0031	0.0036	0.0027	0.0037	0.0021	0.0032	0.0015	0.0044	0.0038
50	0.0067	0.0064	0.0034	0.0028	0.0033	0.0024	0.0030	0.0021	0.0031	0.0017	0.0027	0.0011	0.0037	0.0031
60	0.0058	0.0055	0.0029	0.0023	0.0028	0.0019	0.0026	0.0017	0.0027	0.0013	0.0023	0.0008	0.0033	0.0026
80	0.0046	0.0043	0.0023	0.0018	0.0023	0.0014	0.0021	0.0013	0.0022	0.0009	0.0019	0.0004	0.0026	0.0020
100	0.0039	0.0035	0.0020	0.0015	0.0019	0.0012	0.0018	0.0010	0.0018	0.0008	0.0016	0.0004	0.0022	0.0016

To allow for the loss of energy in the form of bremsstrahlung it is necessary to use the bremsstrahlung correction factors $\zeta(T_0)$, illustrated in Figure 2, to weight the intensity $g''(h\nu')$ in equation (29). When this is done the cross section ${}_e\sigma_a$ is given by the equation

$${}_e\sigma_a = \int_{h\nu/(1+2\alpha)}^{h\nu} \frac{h\nu - h\nu'}{h\nu} \zeta(h\nu - h\nu') g(h\nu') d(h\nu'), \quad (31)$$

which must be evaluated numerically.

In the present work, for purposes of comparison, values of ${}_e\sigma_a$ were calculated from both equations (30) and (31). The two sets of results for the various materials dealt with in this paper are given in mass units in columns (a) and (b) respectively of Table 3. The results for air were derived from those for nitrogen, oxygen, and argon. This table shows that for heavy materials and high energies the value of the Compton absorption coefficient is substantially reduced when bremsstrahlung is taken into account. Thus for aluminium and primary energies of 1, 10, and 100 MeV the new values (equation (31)) are about 100, 94, and 63% respectively of the Klein-Nishina values (equation (30)). For lead and the same energies these percentages are about 98, 75, and 25 respectively.

V. PAIR PRODUCTION ABSORPTION COEFFICIENT

In this section values of the pair production absorption coefficient are derived from those for the attenuation coefficient given by Grodstein (see Table 4), by applying corrections for the escape of energy in the form of bremsstrahlung and annihilation radiation.

In the pair production process a portion $2\mu_0$ of the energy of the incident photon is converted into a positron and an electron, and the remaining energy is shared, not necessarily equally, between these two particles in the form of kinetic energy. The attenuation coefficient ${}_a\kappa$ is determined by integrating the cross section $\varphi(E_+)dE_+$ for the creation of a positron with a total energy between E_+ and $E_+ + dE_+$, and an electron with corresponding energy between E_- and $E_- - dE_-$, over all possible energies of the positron. Thus

$${}_a\kappa = \int_{\mu_0}^{h\nu - \mu_0} \varphi(E_+) dE_+. \quad (32)$$

For the present determination of the absorption coefficient ${}_a\kappa_a$, bremsstrahlung energy losses were taken into account by using the bremsstrahlung correction factors (see Fig. 2) to weight the intensity $\varphi(E_+)$ in equation (32). Thus

$$\begin{aligned} {}_a\kappa_a &= \int_{\mu_0}^{h\nu - \mu_0} \frac{\zeta(E_+ - \mu_0)E_+ + \zeta(E_- - \mu_0)E_-}{h\nu} \varphi(E_+) dE_+ \\ &= \frac{2}{h\nu} \int_{\mu_0}^{h\nu - \mu_0} \zeta(E_+ - \mu_0)E_+ \varphi(E_+) dE_+. \end{aligned} \quad (33)$$

When the primary energy is sufficiently low for the radiation energy loss to be negligible compared to the ionization energy loss, $\zeta(E_+ - \mu_0) = \zeta(E_- - \mu_0) = 1$ and equation (33) reduces to equation (32).

TABLE 4
PAIR PRODUCTION MASS ATTENUATION AND ABSORPTION COEFFICIENTS, κ/ρ AND κ_a/ρ *
Units are cm^2/g

Energy (MeV)	Hydrogen		Nitrogen		Oxygen		Aluminium		Argon	
	κ/ρ	κ_a/ρ	κ/ρ	κ_a/ρ	κ/ρ	κ_a/ρ	κ/ρ	κ_a/ρ	κ/ρ	κ_a/ρ
1.5	0.0000	0.0000	0.0001	0.0000	0.0001	0.0000	0.0002	0.0001	0.0002	0.0001
2.0	0.0001	0.0001	0.0004	0.0002	0.0004	0.0002	0.0007	0.0003	0.0009	0.0004
3.0	0.0003	0.0002	0.0011	0.0007	0.0012	0.0008	0.0019	0.0013	0.0026	0.0017
4.0	0.0005	0.0004	0.0017	0.0013	0.0020	0.0015	0.0031	0.0023	0.0041	0.0029
5.0	0.0007	0.0005	0.0024	0.0019	0.0027	0.0021	0.0042	0.0033	0.0055	0.0040
6.0	0.0009	0.0007	0.0029	0.0024	0.0033	0.0028	0.0051	0.0042	0.0067	0.0050
8.0	0.0013	0.0011	0.0038	0.0034	0.0043	0.0038	0.0067	0.0058	0.0086	0.0070
10	0.0016	0.0014	0.0046	0.0040	0.0052	0.0046	0.0081	0.0069	0.0103	0.0087
15	0.0023	0.0020	0.0061	0.0056	0.0069	0.0061	0.0106	0.0092	0.0134	0.0117
20	0.0029	0.0026	0.0072	0.0067	0.0082	0.0073	0.0125	0.0107	0.0158	0.0135
30	0.0036	0.0034	0.0088	0.0079	0.0100	0.0087	0.0150	0.0125	0.0191	0.0155
40	0.0042	0.0039	0.0099	0.0086	0.0113	0.0096	0.0169	0.0135	0.0214	0.0166
50	0.0046	0.0043	0.0108	0.0092	0.0122	0.0101	0.0183	0.0140	0.0231	0.0171
60	0.0050	0.0047	0.0115	0.0095	0.0129	0.0105	0.0194	0.0142	0.0246	0.0174
80	0.0056	0.0052	0.0125	0.0100	0.0141	0.0110	0.0211	0.0145	0.0265	0.0175
100	0.0060	0.0056	0.0133	0.0104	0.0150	0.0112	0.0223	0.0144	0.0280	0.0174
	Iron		Lead		Air		Water			
	κ/ρ	κ_a/ρ	κ/ρ	κ_a/ρ	κ/ρ	κ_a/ρ	κ/ρ	κ_a/ρ		
1.5	0.0003	0.0001	0.0016	0.0003	0.0001	0.0000	0.0001	0.0000		
2.0	0.0013	0.0005	0.0050	0.0015	0.0004	0.0002	0.0004	0.0002		
3.0	0.0038	0.0022	0.0114	0.0061	0.0011	0.0008	0.0011	0.0007		
4.0	0.0060	0.0041	0.0168	0.0103	0.0018	0.0014	0.0019	0.0014		
5.0	0.0081	0.0059	0.0211	0.0135	0.0025	0.0019	0.0024	0.0019		
6.0	0.0099	0.0076	0.0247	0.0170	0.0030	0.0025	0.0030	0.0025		
8.0	0.0127	0.0104	0.0306	0.0220	0.0040	0.0035	0.0040	0.0034		
10	0.0152	0.0124	0.0359	0.0257	0.0048	0.0043	0.0048	0.0042		
15	0.0198	0.0159	0.0459	0.0306	0.0064	0.0058	0.0064	0.0058		
20	0.0231	0.0180	0.0536	0.0333	0.0075	0.0069	0.0076	0.0067		
30	0.0277	0.0204	0.0642	0.0353	0.0092	0.0082	0.0092	0.0082		
40	0.0310	0.0214	0.0715	0.0356	0.0104	0.0090	0.0103	0.0090		
50	0.0335	0.0217	0.0769	0.0355	0.0113	0.0095	0.0112	0.0096		
60	0.0355	0.0218	0.0813	0.0350	0.0120	0.0098	0.0119	0.0100		
80	0.0384	0.0215	0.0875	0.0330	0.0130	0.0104	0.0130	0.0105		
100	0.0404	0.0208	0.0920	0.0297	0.0139	0.0107	0.0138	0.0108		

* Values of κ/ρ are from Grodstein (1957).

The cross section $\varphi(E_+)dE_+$ required in equations (32) and (33) has been derived by Bethe and Heitler (1934) for the case of pair production in the field of the nucleus. Their results, which are analogous to equations (2), (3), and (4) for the bremsstrahlung, are

$$\gamma_p \gg 1, \quad \varphi(E_+)dE_+ = \frac{4r_0^2 Z^2}{137(h\nu)^3} (E_+^2 + E_-^2 + \frac{2}{3}E_+E_-) \left(\ln \frac{2E_+E_-}{h\nu\mu_0} - \frac{1}{2} \right) dE_+, \quad (34)$$

$$2 < \gamma_p < 15, \quad \varphi(E_+)dE_+ = \frac{4r_0^2 Z^2}{137(h\nu)^3} (E_+^2 + E_-^2 + \frac{2}{3}E_+E_-) \left[\ln \frac{2E_+E_-}{h\nu\mu_0} - \frac{1}{2} - c(\gamma_p) \right] dE_+, \quad (35)$$

and

$$\gamma_p < 2, \quad \varphi(E_+)dE_+ = \frac{4r_0^2 Z^2}{137(h\nu)^3} \left\{ (E_+^2 + E_-^2) \left[\frac{\varphi_1(\gamma_p)}{4} - \frac{\ln Z}{3} \right] + \frac{2}{3}E_+E_- \left[\frac{\varphi_2(\gamma_p)}{4} - \frac{\ln Z}{3} \right] \right\} dE_+. \quad (36)$$

where $\gamma_p = 100h\nu\mu_0/E_+E_-Z^{1/3}$ is a measure of the screening. For complete screening $\gamma_p = 0$ and the expression in the braces of equation (36) reduces to

$$\{(E_+^2 + E_-^2 + 2E_+E_-/3) \ln (183Z^{-1/3}) - E_+E_-/9\}.$$

Using equations (34), (35), and (36) to obtain $\varphi(E_+)$, the weighted intensity $\varphi(E_+)\zeta(E_+ - \mu_0)E_+$ was determined for each material and ${}_a\kappa_a$ calculated from equation (33) by numerical integration. In the case of water, equation (33) was evaluated using values of the bremsstrahlung correction factor for this material, and values of the intensity $\varphi(E_+)$ given by $2\varphi_H(E_+) + \varphi_O(E_+)$, where $\varphi_H(E_+)$ and $\varphi_O(E_+)$ are the intensities for hydrogen and oxygen. The results for the weighted intensity for hydrogen, aluminium, and lead are shown graphically in Figure 5 for various primary energies. For convenience the intensity is plotted as a function of $(E_+ - \mu_0)/(h\nu - 2\mu_0)$ rather than of E_+ .

The results for ${}_a\kappa_a$ must be corrected for the Born approximation and also for the fact that pair production occurs in the field of the atomic electrons. These corrections were made with the aid of Grodstein's published results for the pair production cross sections in the fields of the nucleus and the atomic electrons, ${}_a\kappa'$ and ${}_a\kappa''$ respectively. Grodstein's results for ${}_a\kappa'$ include a correction ${}_a\kappa'_{\text{Born}}$ for the Born approximation given by the equation

$${}_a\kappa'_{\text{Born}} = -\Delta\sigma_c + (a^2\mu_0/h\nu) \ln (h\nu/\mu_0), \quad (37)$$

where $\Delta\sigma_c$ and a^2 are functions of Z given in her Table 7. A corresponding correction was therefore made in the present work by multiplying the values of ${}_a\kappa_a$ from equation (33) by the factor ${}_a\kappa'/({}_a\kappa' - {}_a\kappa'_{\text{Born}})$. To allow for pair production in the field of the atomic electrons the resulting values were multiplied by $({}_a\kappa' + {}_a\kappa'')/{}_a\kappa'$.

As stated in the introduction, the annihilation radiation correction is very large at energies of a few MeV. In order to obtain accurate values of the pair absorption coefficient this energy loss was taken into account in the present work by subtracting the amount $(2\mu_0/h\nu){}_a\kappa$ from the values of ${}_a\kappa_a$ obtained above, where ${}_a\kappa = {}_a\kappa' + {}_a\kappa''$ is the total Grodstein pair attenuation coefficient.

The final results for the pair production absorption coefficient for the various materials dealt with in this paper are given in Table 4. The results for air were derived from those for nitrogen, oxygen, and argon. Reference to this table shows the effect of taking bremsstrahlung and annihilation radiation into account. For example, for hydrogen, iron, and lead and 10 MeV radiation, the pair production absorption coefficients are respectively only about 88, 82, and 72% of the attenuation coefficients. For 100 MeV radiation these percentages become about 93, 52, and 32 respectively.

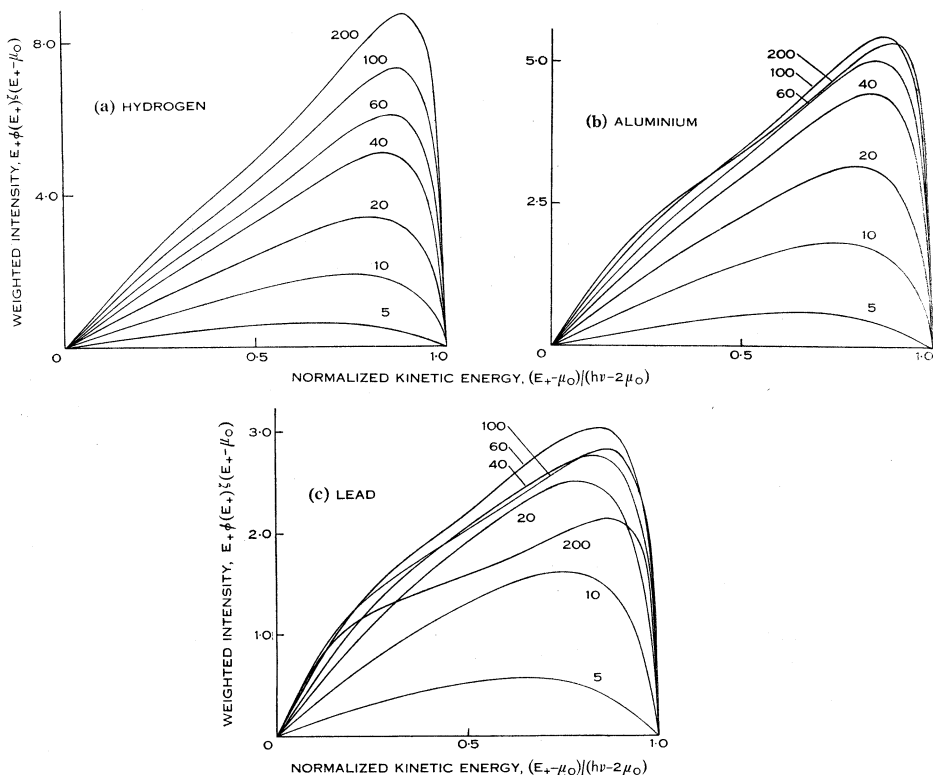


Fig. 5.—Intensity distribution of pair production positrons weighted to allow for bremsstrahlung energy losses. (The ordinates are in units of $2r_0^2 Z^2 / 137 h\nu$, E_+ is the total energy of the positron, and the numbers affixed to the curves refer to the primary radiation energy $h\nu$ in units of $\mu_0 = m_0 c^2$).

VI. TOTAL ABSORPTION COEFFICIENT

Addition of the photoelectric, Compton, and pair production absorption coefficients determined in the previous section by taking into account the loss of energy from the material in the form of fluorescent and annihilation radiation and bremsstrahlung, in addition to Compton-scattered radiation, gives the new values for the total absorption coefficient listed in Table 5.

It is interesting to compare these results with values obtained from equation (1), which allows for the Compton-scattered radiation only. For this

purpose the work of Evans (1955), which was based on the tables of atomic cross sections given by White (1952), was extended to include the various materials dealt with in this paper and revised using the more recent tables of τ and κ given by Grodstein (1957) and McGinnies (1959) (see Tables 2 (a) and 2 (b) and Table 4) together with values of σ_a calculated from the Klein-Nishina equation (see columns (a) of Table 3). The revised values, given in columns (a) of Table 5, differ from those of Evans at low energies because the values of τ given by McGinnies are substantially greater than those given by White; for example, for lead and an energy of 0.01 MeV the revised value is about 70% greater than Evans's value. Values of the total mass attenuation given by Grodstein and McGinnies are also included in Table 5.

TABLE 5

TOTAL MASS ATTENUATION AND ABSORPTION COEFFICIENTS μ/ρ AND μ_a/ρ^*

The two sets of values for the absorption coefficient allow for the escape from the material of (a) scattered radiation only and (b) all secondary radiations. Units are cm^2/g

Energy (MeV)	Hydrogen		Nitrogen			Oxygen			Aluminium			
	μ/ρ	μ_a/ρ	μ/ρ	μ_a/ρ	μ/ρ	μ_a/ρ	μ/ρ	μ_a/ρ	μ/ρ	μ_a/ρ		
		(a) (b)	(a) (b)	(a) (b)	(a) (b)	(a) (b)	(a) (b)	(a) (b)	(a) (b)			
0.01	0.385	0.0099	0.0099	3.50	3.32	3.32	5.54	5.35	5.35	25.8	25.6	25.6
0.015	0.377	0.0111	0.0111	1.07	0.882	0.882	1.63	1.44	1.44	7.67	7.48	7.48
0.02	0.369	0.0133	0.0133	0.531	0.352	0.352	0.747	0.568	0.568	3.22	3.04	3.04
0.03	0.357	0.0186	0.0186	0.271	0.101	0.101	0.332	0.161	0.161	1.03	0.864	0.864
0.04	0.345	0.0231	0.0231	0.208	0.0456	0.0456	0.230	0.0674	0.0674	0.492	0.335	0.335
0.05	0.335	0.0271	0.0271	0.185	0.0295	0.0295	0.195	0.0399	0.0399	0.319	0.170	0.170
0.06	0.326	0.0305	0.0305	0.173	0.0240	0.0240	0.179	0.0301	0.0301	0.246	0.102	0.102
0.08	0.309	0.0362	0.0362	0.159	0.0217	0.0217	0.162	0.0239	0.0239	0.185	0.0527	0.0527
0.10	0.295	0.0406	0.0406	0.150	0.0222	0.0222	0.151	0.0231	0.0231	0.160	0.0369	0.0369
0.15	0.265	0.0481	0.0481	0.134	0.0246	0.0246	0.134	0.0250	0.0250	0.134	0.0281	0.0281
0.20	0.243	0.0525	0.0525	0.123	0.0265	0.0265	0.123	0.0269	0.0269	0.120	0.0273	0.0273
0.30	0.212	0.0569	0.0569	0.106	0.0287	0.0287	0.107	0.0287	0.0287	0.103	0.0281	0.0281
0.40	0.189	0.0586	0.0586	0.0955	0.0295	0.0295	0.0953	0.0295	0.0295	0.0922	0.0287	0.0287
0.50	0.173	0.0590	0.0590	0.0869	0.0297	0.0297	0.0870	0.0297	0.0297	0.0840	0.0286	0.0286
0.60	0.160	0.0587	0.0587	0.0805	0.0296	0.0296	0.0806	0.0296	0.0296	0.0777	0.0285	0.0285
0.80	0.140	0.0574	0.0574	0.0707	0.0289	0.0289	0.0708	0.0289	0.0289	0.0683	0.0279	0.0279
1.0	0.126	0.0555	0.0555	0.0636	0.0280	0.0280	0.0636	0.0280	0.0280	0.0614	0.0270	0.0269
1.5	0.103	0.0507	0.0507	0.0517	0.0256	0.0255	0.0518	0.0257	0.0255	0.0500	0.0248	0.0246
2.0	0.0876	0.0465	0.0465	0.0445	0.0238	0.0238	0.0445	0.0238	0.0236	0.0432	0.0232	0.0227
3.0	0.0691	0.0399	0.0399	0.0357	0.0211	0.0206	0.0359	0.0212	0.0207	0.0353	0.0212	0.0203
4.0	0.0579	0.0353	0.0353	0.0306	0.0193	0.0187	0.0309	0.0196	0.0189	0.0310	0.0200	0.0189
5.0	0.0502	0.0318	0.0316	0.0273	0.0180	0.0174	0.0276	0.0183	0.0177	0.0282	0.0193	0.0180
6.0	0.0446	0.0291	0.0289	0.0249	0.0171	0.0164	0.0254	0.0175	0.0167	0.0264	0.0188	0.0174
8.0	0.0371	0.0252	0.0248	0.0218	0.0159	0.0152	0.0224	0.0164	0.0156	0.0241	0.0183	0.0168
10	0.0321	0.0224	0.0222	0.0200	0.0151	0.0143	0.0206	0.0157	0.0148	0.0229	0.0182	0.0164
15	0.0249	0.0183	0.0179	0.0175	0.0142	0.0131	0.0183	0.0149	0.0136	0.0215	0.0183	0.0163
20	0.0209	0.0160	0.0156	0.0163	0.0139	0.0128	0.0173	0.0148	0.0135	0.0212	0.0188	0.0162
30	0.0168	0.0135	0.0130	0.0154	0.0138	0.0123	0.0166	0.0149	0.0131	0.0214	0.0198	0.0164
40	0.0147	0.0121	0.0116	0.0152	0.0139	0.0121	0.0165	0.0152	0.0130	0.0220	0.0208	0.0166
50	0.0133	0.0113	0.0107	0.0152	0.0142	0.0119	0.0165	0.0156	0.0129	0.0225	0.0216	0.0164
60	0.0125	0.0108	0.0102	0.0153	0.0144	0.0118	0.0167	0.0159	0.0129	0.0231	0.0222	0.0161
80	0.0115	0.0103	0.0095	0.0154	0.0148	0.0118	0.0171	0.0164	0.0127	0.0240	0.0233	0.0159
100	0.0109	0.0099	0.0092	0.0158	0.0153	0.0119	0.0175	0.0169	0.0127	0.0247	0.0242	0.0156

* Values of μ/ρ are from Grodstein (1957) and McGinnies (1959).

TABLE 5 (Continued)

Energy (MeV)	Argon			Iron			Lead†			Air			Water		
	μ/ρ		μ_a/ρ	μ/ρ		μ_a/ρ	μ/ρ		μ_a/ρ	μ/ρ		μ_a/ρ	μ/ρ		μ_a/ρ
	(a)	(b)	(a)	(b)	(a)	(b)	(a)	(b)	(a)	(b)	(a)	(b)	(a)	(b)	
0.01	64.0	64.0	62.0	179	179	141	137	137	137	4.76	4.56	4.56	4.96	4.75	4.75
0.01307							67.6	67.6	67.6						
0.015	19.6	19.6	19.2	57.7	57.7	49.4				1.44	1.25	1.25	1.49	1.28	1.28
0.01589							168	168	115						
0.02	8.36	8.20	8.07	25.0	25.0	22.2	90	90	68.1	0.683	0.501	0.501	0.705	0.506	0.506
0.03	2.59	2.44	2.41	7.91	7.75	7.20	30.6	30.5	25.7	0.315	0.144	0.144	0.335	0.146	0.146
0.04	1.09	0.946	0.939	3.46	3.31	3.14	14.3	14.2	12.5	0.225	0.0620	0.0620	0.243	0.0624	0.0624
0.05	0.612	0.472	0.469	1.80	1.65	1.59	7.96	7.83	7.10	0.193	0.0375	0.0375	0.211	0.0385	0.0385
0.06	0.412	0.278	0.276	1.11	0.975	0.940	4.72	4.60	4.25	0.177	0.0286	0.0286	0.196	0.0301	0.0301
0.08	0.247	0.124	0.124	0.550	0.421	0.411	2.12	2.01	1.89	0.161	0.0235	0.0235	0.178	0.0253	0.0253
0.08823							1.64	1.54	1.46						
							7.42	7.32	1.38						
0.10	0.188	0.0725	0.0725	0.342	0.224	0.219	5.29	5.19	1.51	0.151	0.0231	0.0231	0.167	0.0251	0.0251
0.15	0.135	0.0367	0.0367	0.183	0.0808	0.0797	1.84	1.753	0.906	0.134	0.0249	0.0249	0.149	0.0276	0.0276
0.20	0.117	0.0301	0.0301	0.138	0.0487	0.0485	0.896	0.820	0.522	0.123	0.0267	0.0267	0.136	0.0297	0.0297
0.30	0.0977	0.0277	0.0277	0.106	0.0338	0.0338	0.356	0.295	0.226	0.106	0.0287	0.0287	0.118	0.0319	0.0319
0.40	0.0867	0.0274	0.0274	0.0919	0.0306	0.0306	0.208	0.156	0.131	0.0953	0.0295	0.0295	0.106	0.0328	0.0328
0.50	0.0790	0.0272	0.0272	0.0828	0.0294	0.0294	0.145	0.0994	0.0876	0.0868	0.0297	0.0297	0.0966	0.0330	0.0330
0.60	0.0730	0.0270	0.0270	0.0762	0.0287	0.0287	0.114	0.0737	0.0669	0.0804	0.0296	0.0296	0.0896	0.0329	0.0329
0.80	0.0638	0.0261	0.0261	0.0664	0.0275	0.0275	0.0836	0.0505	0.0471	0.0706	0.0289	0.0289	0.0786	0.0321	0.0321
1.0	0.0573	0.0252	0.0252	0.0595	0.0263	0.0263	0.0684	0.0402	0.0378	0.0635	0.0280	0.0280	0.0706	0.0311	0.0311
1.5	0.0468	0.0233	0.0231	0.0485	0.0241	0.0238	0.0512	0.0306	0.0279	0.0517	0.0256	0.0255	0.0575	0.0285	0.0284
2.0	0.0407	0.0220	0.0214	0.0424	0.0231	0.0220	0.0457	0.0293	0.0242	0.0445	0.0238	0.0235	0.0493	0.0263	0.0262
3.0	0.0338	0.0206	0.0194	0.0360	0.0224	0.0205	0.0421	0.0305	0.0238	0.0357	0.0211	0.0206	0.0396	0.0233	0.0228
4.0	0.0301	0.0199	0.0184	0.0330	0.0224	0.0198	0.0420	0.0330	0.0249	0.0307	0.0194	0.0188	0.0339	0.0213	0.0207
5.0	0.0279	0.0196	0.0176	0.0313	0.0227	0.0198	0.0426	0.0353	0.0258	0.0274	0.0181	0.0174	0.0301	0.0198	0.0191
6.0	0.0266	0.0195	0.0173	0.0304	0.0231	0.0201	0.0436	0.0374	0.0278	0.0250	0.0172	0.0165	0.0275	0.0188	0.0181
8.0	0.0248	0.0194	0.0174	0.0295	0.0239	0.0207	0.0459	0.0412	0.0305	0.0220	0.0160	0.0153	0.0240	0.0173	0.0165
10	0.0241	0.0197	0.0176	0.0294	0.0249	0.0212	0.0489	0.0450	0.0324	0.0202	0.0154	0.0145	0.0219	0.0165	0.0155
15	0.0237	0.0207	0.0183	0.0304	0.0273	0.0223	0.0554	0.0527	0.0352	0.0178	0.0145	0.0132	0.0190	0.0153	0.0141
20	0.0240	0.0218	0.0187	0.0315	0.0292	0.0230	0.0611	0.0592	0.0367	0.0166	0.0141	0.0131	0.0177	0.0149	0.0136
30	0.0251	0.0236	0.0192	0.0339	0.0324	0.0236	0.0697	0.0683	0.0375	0.0158	0.0141	0.0126	0.0166	0.0147	0.0131
40	0.0261	0.0250	0.0192	0.0359	0.0347	0.0235	0.0759	0.0749	0.0372	0.0156	0.0143	0.0124	0.0162	0.0148	0.0128
50	0.0271	0.0262	0.0192	0.0376	0.0366	0.0234	0.0805	0.0797	0.0366	0.0157	0.0147	0.0122	0.0161	0.0150	0.0126
60	0.0280	0.0272	0.0190	0.0391	0.0383	0.0230	0.0843	0.0836	0.0357	0.0158	0.0148	0.0122	0.0161	0.0151	0.0125
80	0.0292	0.0286	0.0188	0.0412	0.0405	0.0233	0.0899	0.0894	0.0334	0.0160	0.0154	0.0121	0.0163	0.0156	0.0125
100	0.0302	0.0298	0.0184	0.0427	0.0423	0.0217	0.0939	0.0936	0.0301	0.0164	0.0159	0.0121	0.0166	0.0160	0.0124

† For this material the values given for 0.01 and 0.01307 MeV (L_{α} edge) are for the M shell; from 0.01589 MeV (L_{β} edge) to 0.08823 MeV (K edge) they are for the L and M shells; and from 0.08823 MeV upwards they are for the K , L , and M shells.

For low energies and heavy materials the values of the absorption coefficients in columns (b) of Table 5 are appreciably less than those in columns (a) owing to taking fluorescent radiation into account. For example, for an energy of 0.01 MeV the column (b) values are about 97 and 79% of the column (a) values for argon and iron respectively. For lead, and energies just above the L_1 and K absorption edges, these proportions fall to about 68 and 19% respectively. At high energies the effect of taking bremsstrahlung into consideration is evident. For example, for an energy of 10 MeV the column (b) values are about 99, 95, 90, 85, and 72% of the column (a) values for hydrogen, nitrogen, aluminium, iron, and lead respectively. For an energy of 100 MeV and the same materials these proportions are about 93, 78, 64, 51, and 32% respectively.

VII. ACKNOWLEDGMENTS

The author is grateful to Mr. R. G. Ackland for his valuable assistance in the preparation of this paper. Thanks are also due to Miss N. Rushford for carrying out many of the calculations.

This paper is published with the permission of the Chief Scientist, Australian Defence Scientific Service, Department of Supply, Melbourne, Australia.

VIII. REFERENCES

- BAKKER, C. J., and SEGRÈ, E. (1951).—*Phys. Rev.* **81** : 489–92.
- BETHE, H. A., and ASHKIN, J. (1953).—“Experimental Nuclear Physics.” (Ed. E. Segrè.) Vol. I, Part II. (Wiley : New York.)
- BETHE, H. A., and HEITLER, W. (1934).—*Proc. Roy. Soc. A* **146** : 83–112.
- BORSELLINO, A. (1947).—*Nuovo Cim.* **4** : 112 ; *Rev. univ. nac. Tucumán A* **6** : 7. (Ref. from “Experimental Nuclear Physics.” (Ed. E. Segrè.) Vol. I, p. 261. (Wiley : New York.))
- BROYLES, C. D., THOMAS, D. A., and HAYNES, S. K. (1953).—*Phys. Rev.* **89** : 715–24.
- BURHOP, E. H. S. (1954).—“The Auger Effect and Other Radiationless Transitions.” (Cambridge Univ. Press.)
- DAVIES, H., and BETHE, H. A. (1952).—*Phys. Rev.* **87** : 156–7.
- EVANS, R. D. (1955).—“The Atomic Nucleus.” (McGraw-Hill : New York.)
- EVANS, R. D., and EVANS, R. O. (1948).—*Rev. Mod. Phys.* **20** : 305–26.
- FANO, U. (1953).—*Nucleonics* **11** : 8–12.
- GRODSTEIN, G. W. (1957).—X-ray attenuation coefficients from 10 keV to 100 MeV. Circ. Nat. Bur. Stand. 583.
- HALL, H. (1936).—*Rev. Mod. Phys.* **8** : 358–97.
- HEITLER, W. (1954).—“The Quantum Theory of Radiation.” 3rd Ed. (Oxford Univ. Press.)
- HILL, R. D., CHURCH, E. L., and MIHELICH, J. W. (1952).—*Rev. Sci. Instrum.* **23** : 523–8.
- HINE, G. J., and BROWNELL, G. L. (1956).—“Radiation Dosimetry.” (Academic Press : New York.)
- JOSEPH, J., and ROHRLICH, F. (1958).—*Rev. Mod. Phys.* **30** : 354–68.
- KOCH, H. W., and MOTZ, J. W. (1959).—*Rev. Mod. Phys.* **31** : 920–55.
- LAY, H. (1934).—*Z. Phys.* **91** : 533.
- MCGINNIES, R. T. (1959).—X-ray attenuation coefficients from 10 keV to 100 MeV. Circ. Nat. Bur. Stand. 583, Supplement.
- NELMS, A. T. (1953).—Graphs of the Compton energy-angle relationship and the Klein-Nishina formula from 10 keV to 500 MeV. Circ. Nat. Bur. Stand. 542.
- PATRONIS, E. T., BRADEN, C. H., and WYLY, L. D. (1957).—*Phys. Rev.* **105** : 681–2.
- ROBINSON, B. L., and FINK, R. W. (1955).—*Rev. Mod. Phys.* **27** : 424–30.
- STERNHEIMER, R. M. (1952).—*Phys. Rev.* **88** : 851–9.
- WHEELER, J. A., and LAMB, W. E. (1939).—*Phys. Rev.* **55** : 858–62.
- WHEELER, J. A., and LAMB, W. E. (1956).—*Phys. Rev.* **101** : 1836.
- WHITE, G. R. (1952).—X-ray attenuation coefficients from 10 keV to 100 MeV. Nat. Bur. Stand. Rep. No. 1003 (unpublished). (The information in this report has been published in “Beta and Gamma-ray Spectroscopy.” (Ed. K. Seigbahn.) (North-Holland Publishing Co. : Amsterdam, 1955.))

APPENDIX

Broad-beam Attenuation

As a typical example, consider the attenuation of a parallel beam of radiation by a large plane slab of absorber (see Fig. 6). From the geometry it can be seen that the amount of energy which is lost at A from the direct beam crossing the spherical volume element dV , and which is converted into secondary radiation travelling in a forward direction within a conical shell of semivertical angle between θ and $\theta+d\theta$, is just balanced by the amount of secondary radiation directed towards dV from corresponding points B lying in a circle around A .

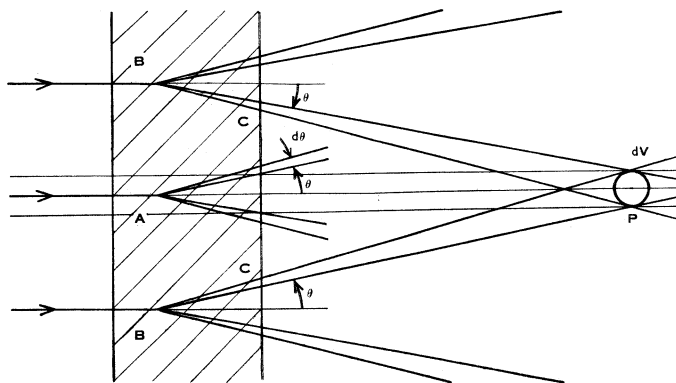


Fig. 6.—Attenuation of a parallel beam of radiation by a plane slab of absorber.

However, since the secondary radiation directed towards dV is attenuated in traversing the distance BC in the absorber, and also since some of the primary energy converted at A into secondary radiation travels in the backwards direction ($\theta \geq \frac{1}{2}\pi$), the total amount of secondary radiation arriving at dV from all points in the absorber must be less than the total amount of direct beam energy converted into secondary radiation. It follows that $\mu_a < \mu_{\text{eff.}} < \mu$. Similar considerations in other examples of broad-beam attenuation give the same result.